

ELECTRONIC SUPPLEMENTARY INFORMATION FOR:

**Liquid Crystalline Copper(I) Complexes with Bright Room
Temperature Phosphorescence**

*Raquel Giménez,^{*a} Olga Crespo,^b Beatriz Diosdado,^b and Anabel Elduque^{*b}*

^a Instituto de Ciencia de Materiales de Aragón (ICMA), Dpto de Química Orgánica, Facultad de Ciencias, Universidad de Zaragoza - CSIC, 50009 Zaragoza, Spain

^b Instituto de Síntesis Química y Catálisis Homogénea (ISQCH), Dpto de Química Inorgánica, Facultad de Ciencias, Universidad de Zaragoza - CSIC, 50009 Zaragoza, Spain.

CONTENT LIST	Page
1. Experimental section	S2
1.1. Materials and methods	S2
1.2. Synthesis and characterization data	S3
2. Additional Tables	S5
Table S1.	S5
3. Additional Figures	S6
Figure S1.	S6
Figure S2.	S6
Figure S3.	S7
Figure S4.	S8
Figure S5.	S9
Figure S6.	S10
Figure S7	S11

1. Experimental section

1.1. Materials and methods

1*H*-pyrazole ligands were prepared following the synthetic route described in H. Blanco, V. Iguarbe, J. Barberá, J. L. Serrano, A. Elduque and R. Giménez, *Chem. Eur. J.*, 2016, **22**, 4924-4930 (Ref 37 in the main text). The synthesis of copper complexes is described in the next section. The copper precursor $[\text{Cu}(\text{MeCN})_4]\text{BF}_4$ and dry triethylamine were commercially available from Sigma Aldrich. Acetone and methanol analytical grade solvents were purchased from Fisher Scientific.

NMR experiments were performed with a Bruker AVANCE 400 spectrometer. Chemical shifts are given in ppm relative to TMS, and the proton-solvent residual peak was used as internal standard (for CD_2Cl_2 $\delta_{\text{H}} = 5.32$ ppm). Infrared spectra were obtained in a Nicolet Avatar 360 FTIR spectrophotometer in the 400–4000 cm^{-1} range. Mass spectra were performed using a Bruker Microflex spectrometer. Elemental analyses were performed using a Perkin-Elmer 2400 series II microanalyzer.

Liquid crystalline behavior and transition temperatures were determined using an Olympus BH-2 polarizing microscope equipped with a Linkam TMS91 hot-stage, a CS196 hot-stage central processor, and a MX-20 camera. DSC measurements were done with a TA Instruments Q-20 calorimeter. Samples were sealed in aluminum pans and a scanning rate of 10 $^{\circ}\text{C min}^{-1}$ under a nitrogen atmosphere was used. X-ray diffraction experiments of the mesophases were performed in a pinhole camera (Anton-Paar) operating with a point focused Ni-filtered Cu-K α beam. Lindemann glass capillaries with 0.9 mm inner diameter were used to contain the sample. The capillary axis was held vertical in a controlled-temperature attachment and the pattern collected on flat photographic film. Bragg's law was used to calculate the *d* spacings.

Single crystal X-ray diffraction data were collected on an Oxford Diffraction Xcalibur diffractometer equipped with a graphite monochromator utilizing MoK α radiation. The diffraction frames were integrated and corrected for absorption using the CrysAlisPro, Agilent Technologies, Version 1.171.36.32. The structure was solved by direct methods. All refinements were carried out using SHELXL-2013 against the F2 data using full-matrix least squares methods. All non-hydrogen atoms were assigned anisotropic displacement parameters and refined without positional constraints except as noted (C29). All hydrogen atoms were constrained to idealized geometries and assigned isotropic displacement parameters 1.2 times the U_{iso} value of their attached carbon atoms (1.5 times for methyl hydrogen atoms). The

CCDC 1980455 contains the supplementary crystallographic data (excluding structure factors).

Neat thin films for luminescence measurements were prepared by drop casting onto quartz plates from dichloromethane solutions. **Cu1** formed less homogeneous films than the liquid crystalline **Cu10** and **Cu14** compounds. Photoluminescent spectra of films were collected in a Jobin-Yvon Horiba Fluorolog FL-3-11 spectrometer using band pathways of 3 nm for both excitation and emission in a solid accessory. Lifetime measurements were recorded with a Fluoromax phosphorimeter accessory containing a UV Xenon flash tube or a 295 nm LED of Horiba Jobin Yvon with pulse duration < 1.2 ns. Quantum Yields were measured by the absolute method using a Hamamatsu Quantaaurus-QY C11347-11 compact one-box absolute quantum yield measurement system. For the quantum yield studies two different films from each sample were measured with two different references in order to analyse the reproducibility of the results. Absolute measurement method has been compared with relative studies of quantum yields for different substances and the relative uncertainties have been calculated as less than 6% [C. Würth, M. Grabolle, J. auli, M. Spieles and U. Resch-Genger, *Anal. Chem.* 2011, **83**, 3431-3439]. Figures 2, S2 and S6a were plotted from spectra obtained with a Hamamatsu Quantaaurus-QY C11347-11, and Figure S5 from the lifetime studies with the flash lamp.

Steady-state photoluminescence spectra in solution (Figure S7) were recorded with a Perkin Elmer LS50 using 1 cm quartz cells.

1.2. Synthesis and characterization data

General procedure for the synthesis of the complexes. A solution of triethylammonium pyrazolate, prepared by reaction of the 1*H*-pyrazole ligand (0.32 mmol) and triethylamine (33 mg, 46 μ L, 0.33 mmol) in acetone (15 mL), was added dropwise to a solution of [Cu(MeCN)₄]BF₄ (100 mg, 0.32 mmol) in acetone (15 mL). The reaction mixture was stirred for 2 h at room temperature under an Argon atmosphere. Then, the reaction mixture was evaporated to dryness and dissolved in dichloromethane (15 mL). The suspension was filtrated through a pad of celite and the solution concentrated almost to dryness. Finally methanol (10 mL) was added to precipitate a white solid, which was separated by filtration, washed with methanol and vacuum-dried.

Cu10. Yield: 80%. ^1H NMR (400 MHz, CD_2Cl_2 , δ , ppm): 6.47 (s, 6H), 4.01-3.92 (m, 18H), 2.42 (s, 18H), 1.87-1.69 (m, 18H), 1.52-1.43 (m, 18H), 1.43-1.22 (m, 108H), 0.93-0.84 (m, 27H). IR (KBr, ν , cm^{-1}): 2955, 2923, 2853 (C-H), 1600, 1579, 1544 (C=N, $\text{C}_{\text{ar}}\text{-C}_{\text{ar}}$), 1246, 1235, 1213, 1115 (C-O). Elemental analysis calc for $\text{C}_{123}\text{H}_{213}\text{Cu}_3\text{N}_6\text{O}_9$: C, 70.0; H, 10.2; N, 4.0 %. Found: C, 69.8; H, 10.2; N, 4.1 %. EM (MALDI⁺, DCTB) m/z: 2110.4 [M^+].

Cu14. Yield: 80%. ^1H NMR (400 MHz, CD_2Cl_2 , δ , ppm): 6.45 (s, 6H), 4.01-3.91 (m, 18H), 2.36 (s, 18H), 1.86-1.70 (m, 18H), 1.52-1.43 (m, 18H), 1.41-1.16 (m, 180H), 0.92-0.84 (m, 27H). IR (KBr, ν , cm^{-1}): 2953, 2919, 2850 (C-H), 1599, 1579, 1547 (C=N, $\text{C}_{\text{ar}}\text{-C}_{\text{ar}}$), 1245, 1235, 1213, 1117 (C-O). Elemental analysis calc for $\text{C}_{159}\text{H}_{285}\text{Cu}_3\text{N}_6\text{O}_9$: C, 73.0; H, 11.0; N, 3.2 %. Found: C, 72.8; H, 10.9; N, 3.2 %. EM (MALDI⁺, DCTB) m/z: 2615.8 [M^+].

Cu1. Yield 88%. ^1H NMR (400 MHz, CD_2Cl_2 , δ , ppm): 6.50 (s, 6H), 3.85 (s, 9H), 3.81 (s, 18H), 2.42 (s, 18H). IR (KBr, ν , cm^{-1}): 2993, 2959, 2937, 2829 (C-H), 1601, 1579, 1530 (C=N, $\text{C}_{\text{ar}}\text{-C}_{\text{ar}}$), 1250, 1235, 1221, 1128, 1107 ($\text{C}_{\text{ar}}\text{-O-C}_{\text{alc}}$). Elemental analysis calc for $\text{C}_{42}\text{H}_{51}\text{Cu}_3\text{N}_6\text{O}_9$: C, 51.8; H, 5.3; N, 8.6 %. Found: C, 51.6; H, 5.3; N, 8.7 %. EM (MALDI⁺, DCTB) m/z: 973.1 [M^+].

2. Additional Tables

Table S1. Crystal data resolution and refinement parameters for **Cu1·CH₂Cl₂**

CCDC number	1980455
Empirical formula	C ₄₃ H ₅₃ Cl ₂ Cu ₃ N ₆ O ₉
Formula mass	1059.43
T /K	150(1)
Wavelength /Å	0.71073
Crystal size /mm	0.80 x 0.03 x 0.02
Crystal system, space group	Monoclinic, P 2 ₁ /n
a, b, c /Å	22.1647(14), 8.2518(4), 27.125(2)
alfa, beta, gamma /°	90, 109.560(7), 90
V /Å ³	4674.8(5)
Z	4
μ /mm ⁻¹	1.526
Theta range for data collection	3.081 to 25.000 deg
Reflections collected / unique	34883 / 8218 [R(int) = 0.1580]
Completeness to theta = 25.000	99.8 %
Data / restraints / parameters	8218 / 5 / 574
Goodness-of-fit on F ²	0.966
Final R indices [I > 2σ(I)]	R1 = 0.0697, wR2 = 0.1401
Largest diff. peak and hole	0.569 and -0.491 e. Å ⁻³

3. Additional Figures

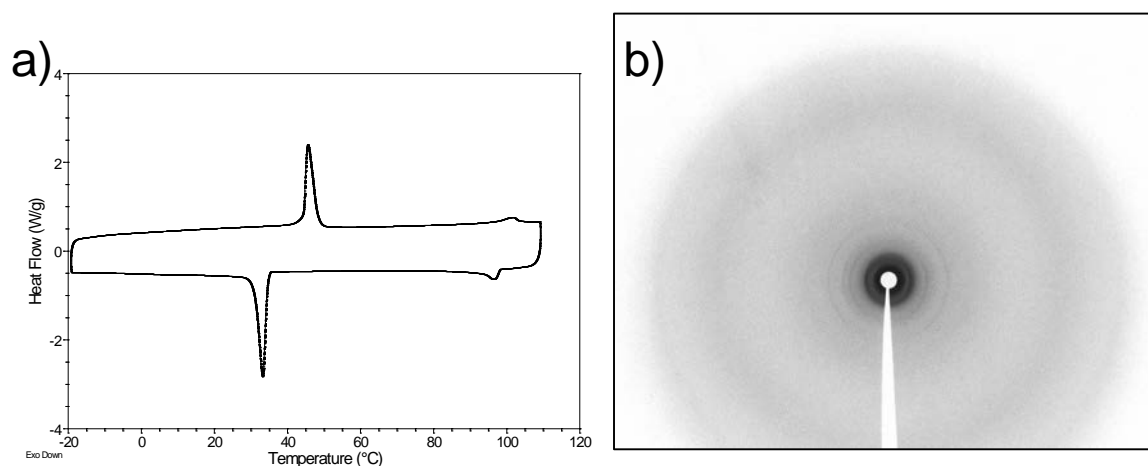


Figure S1. a) DSC thermogram for **Cu14**. b) XRD of the Col_h phase of **Cu14**

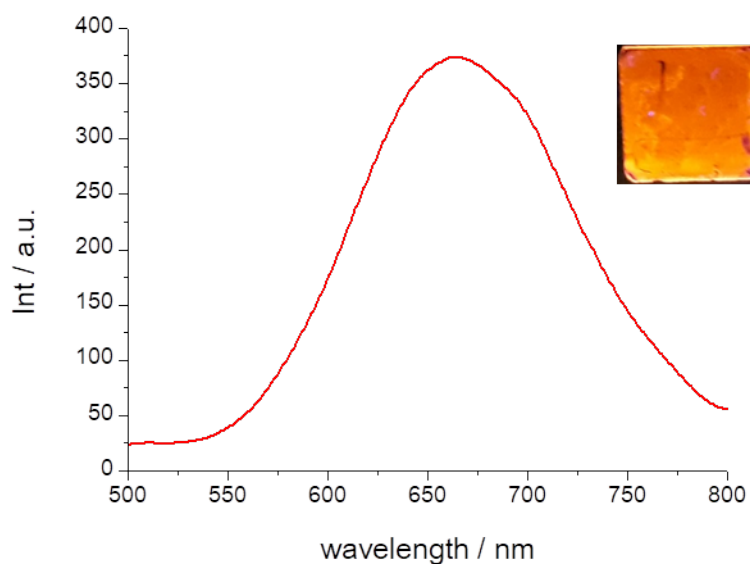
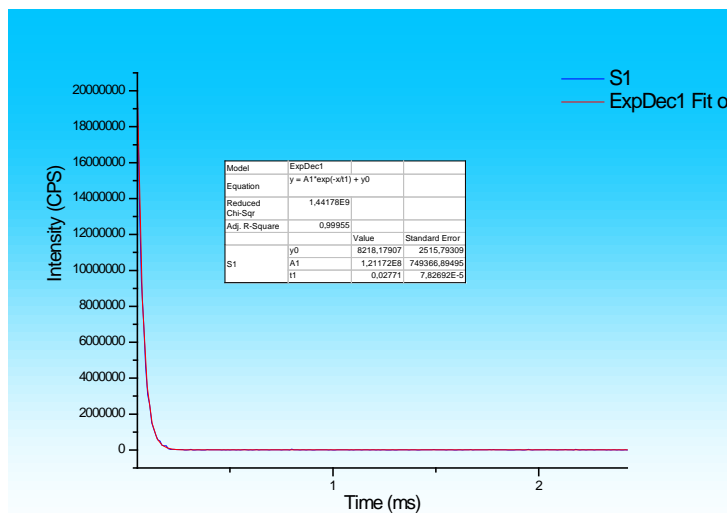
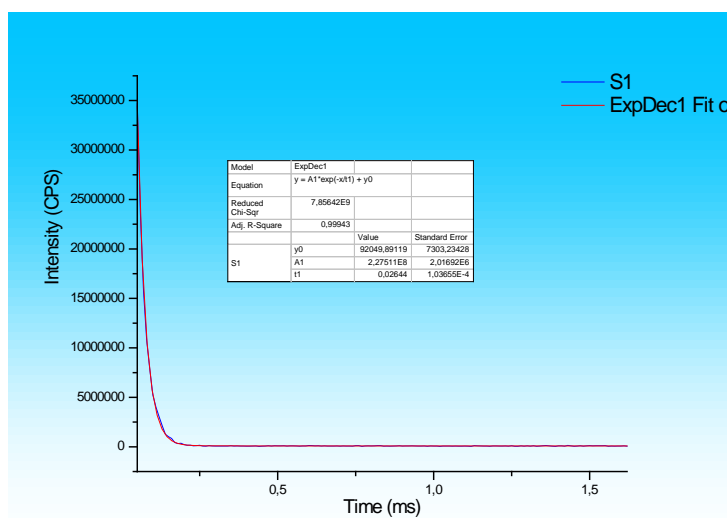


Figure S2. Photoluminescence spectrum for **Cu14** at 25 °C (excitation wavelength 290 nm), and emission of the film observed under irradiation with a 254 nm handheld lamp (overexposed picture, real color is given by CIE 1931 color space coordinates).

a)



b)



c)

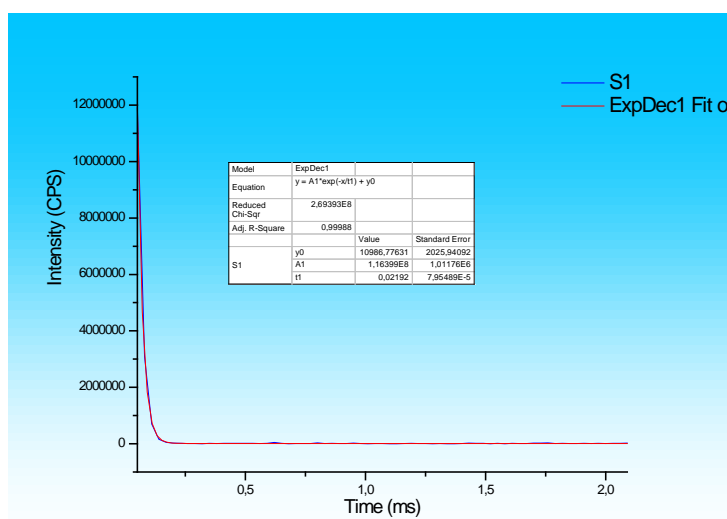
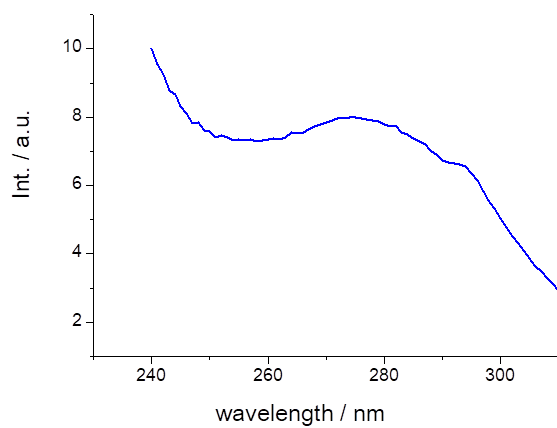
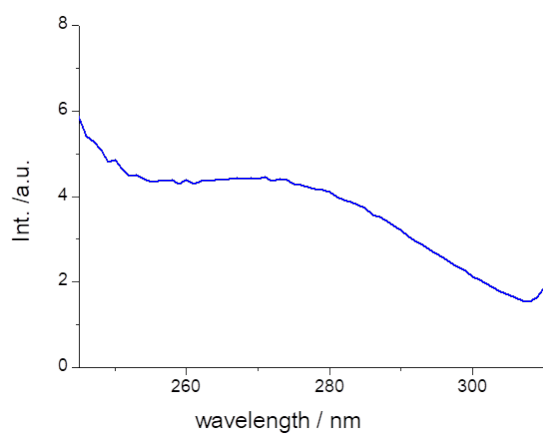


Figure S3. Lifetime experiment and fitting for a) **Cu10** at 25 °C, b) **Cu14** at 25 °C, c) **Cu14** at 50 °C.

a)



b)



c)

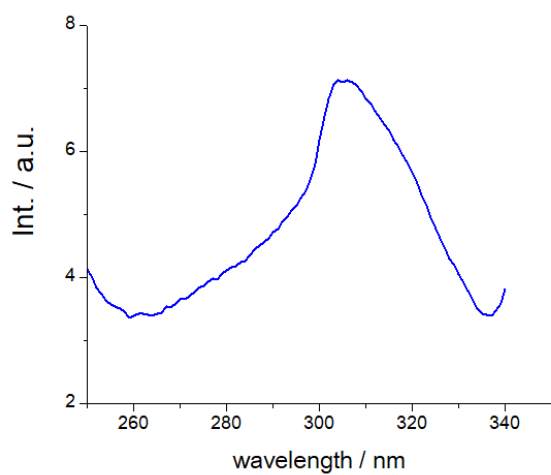


Figure S4. Excitation spectra for a) **Cu10**, b) **Cu14** and c) **Cu1**

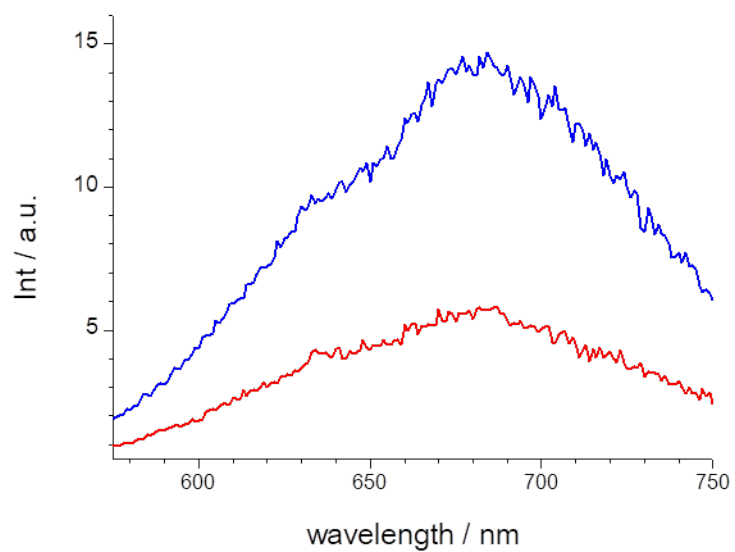
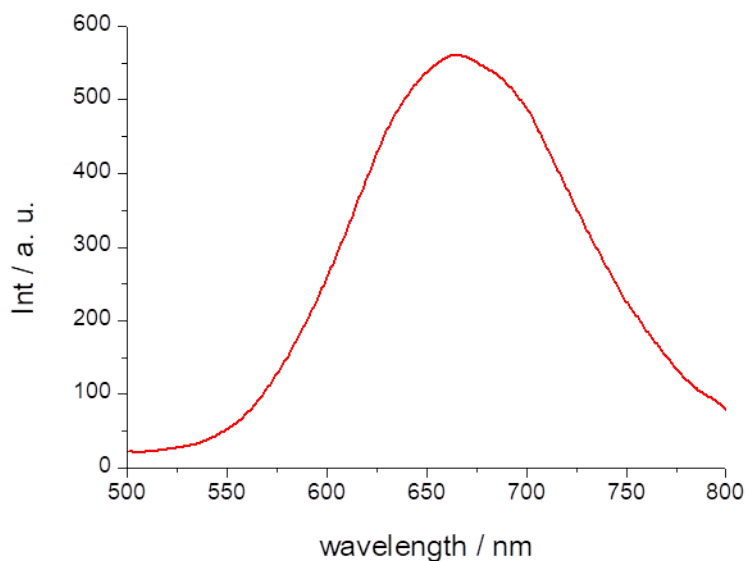


Figure S5. .Photoluminescence spectrum of a film of **Cu14** in two different phases. Blue line crystal phase at 25 °C. Red line: liquid crystal phase at 50 °C (excitation wavelength 290 nm).

a)



b)

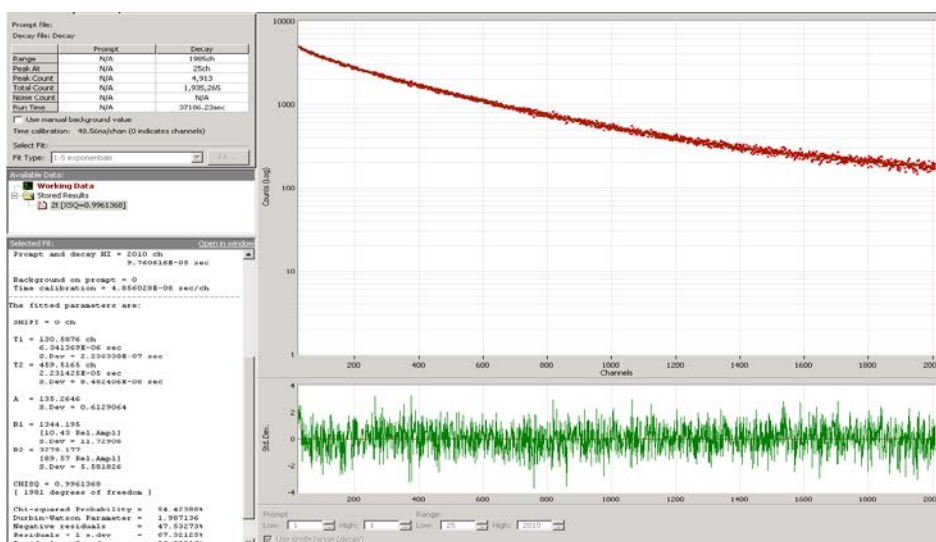
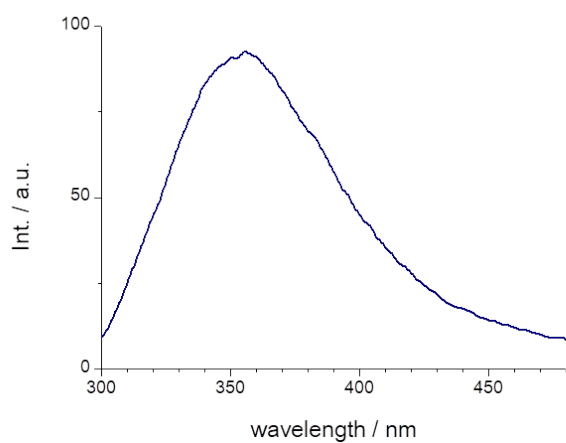
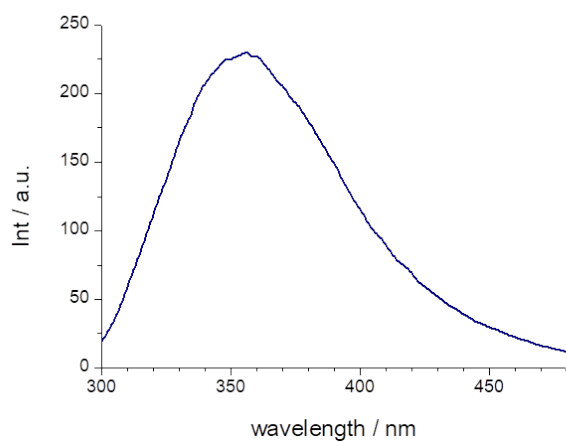


Figure S6. a) Photoluminescence spectrum for **Cu1** at 25 °C (excitation wavelength 290 nm), and emission of the film observed under irradiation with a 254 nm handheld lamp (overexposed picture, real color is given by CIE 1931 color space coordinates). b) lifetime experiment and fitting for **Cu1** at 25 °C

a)



b)



c)

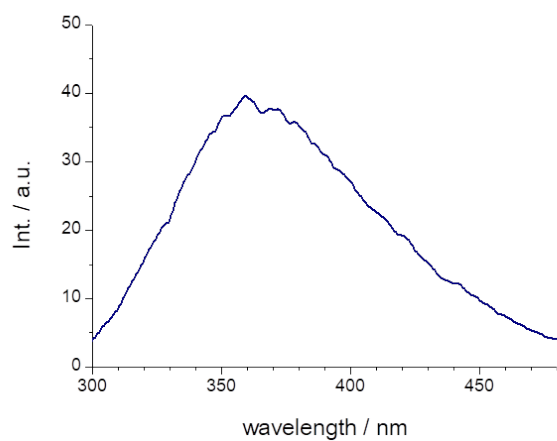


Figure S7. Emission spectra in diluted THF solution for a) **Cu10**, b) **Cu14** and c) **Cu1** (excitation wavelength 256 nm).